doi:10.1093/brain/awz216 BRAIN 2019: 142; 2605–2616 | 2605

BRAIN
A JOURNAL OF NEUROLOGY

Nonsense mutations in alpha-II spectrin in three families with juvenile onset hereditary motor neuropathy

Danique Beijer,[1,2] Tine Deconinck,[1,2] Jan L. De Bleecker,[3] Maria Teresa Dotti,[4] Alessandro Malandrini,[4] J. Andoni Urtizberea,[5] Miren Zulaica,[6,7] Adolfo López de Munain,[6,7] Bob Asselbergh,[8] Peter De Jonghe[1,2,9] and Jonathan Baets[1,2,9]

Distal hereditary motor neuropathies are a rare subgroup of inherited peripheral neuropathies hallmarked by a length-dependent axonal degeneration of lower motor neurons without significant involvement of sensory neurons. We identified patients with heterozygous nonsense mutations in the αII-spectrin gene, *SPTAN1*, in three separate dominant hereditary motor neuropathy families via next-generation sequencing. Variable penetrance was noted for these mutations in two of three families, and phenotype severity differs greatly between patients. The mutant mRNA containing nonsense mutations is broken down by nonsense-mediated decay and leads to reduced protein levels in patient cells. Previously, dominant-negative αII-spectrin gene mutations were described as causal in a spectrum of epilepsy phenotypes.

1 Neurogenetics Group, Center for Molecular Neurology, University of Antwerp, Belgium
2 Laboratory of Neuromuscular Pathology, Institute Born-Bunge, University of Antwerp, Belgium
3 Department of Neurology, University Hospital Ghent, Belgium
4 Department of Medicine, Surgery and Neuroscience, University of Siena, Italy
5 Neuromuscular Reference Center, Hôpital Marin, AP-HP, Hendaye, France
6 Neuroscience Area, Institute Biodonostia, Hospital Universitario Donostia, San Sebastian, Spain
7 Centro de Investigacion Biomedica en Red sobre Enfermedades Neurodegenerativas (CIBERNED), Institute Carlos III, Madrid, Spain
8 VIB-UAntwerp Center for Molecular Neurology, University of Antwerp, Antwerp, Belgium
9 Neuromuscular Reference Centre, Department of Neurology, Antwerp University Hospital, Belgium

Correspondence to: Prof. Dr Jonathan Baets
Neurogenetics Group
Center for Molecular Neurology
University of Antwerp - CDE - Parking 4, Building V
Universiteitsplein 1, B-2610 Wilrijk, Belgium
E-mail: Jonathan.Baets@uantwerpen.vib.be

Keywords: distal hereditary motor neuropathies; next-generation sequencing; nonsense mutations; alpha-II-spectrin

Abbreviations: HMN = hereditary motor neuropathy; NCS = nerve conduction studies; NGS = next-generation sequencing; NMD = nonsense-mediated decay

Received December 6, 2018. Revised April 25, 2019. Accepted May 28, 2019. Advance Access publication July 22, 2019

Introduction

Inherited peripheral neuropathies, the most common type of inherited neuromuscular disease, are a group of disorders with marked clinical and genetic heterogeneity. Hereditary motor neuropathies (HMN) are a rarer subgroup among inherited peripheral neuropathies, causing a length-dependent axonal degeneration of lower motor neurons typically without obvious involvement of sensory neurons. Depending on the subtype, patients may present with distal atrophy and muscle weakness, whereas proximal involvement only develops later in the disease progression. Foot malformations as well as other additional clinical characteristics including pyramidal signs, vocal fold and diaphragm paralysis can be present (Rossor *et al.*, 2012).

The widespread introduction of next-generation sequencing (NGS) techniques over the past decade has allowed for rapid disease gene identification, with currently over 90 inherited peripheral neuropathy-associated genes, as well as detailed investigation of genotype-phenotype correlations. As such it has become clear that the idea of one gene, one phenotype is oversimplified and does not capture the true complexity of most Mendelian diseases. There are numerous examples of distinct phenotypes caused by mutations in different genes, as well as mutations in one gene causing divergent clinical entities sometimes even impacting different organ systems (Boerkoel *et al.*, 2002; Montenegro *et al.*, 2018). One of the more extreme genes is *LMNA*, in which mutations have been described causing Emery-Dreifuss muscular dystrophy, several types of dilated cardiomyopathy, atrial fibrillation, Charcot-Marie-Tooth disease (CMT) and Hutchinson-Gilford progeria (Tazir *et al.*, 2013; Montenegro *et al.*, 2018). HMN has been shown to display similar genetic pleiotropy, by genetic overlap with other neuromuscular disorders such as amyotrophic lateral sclerosis (ALS) and congenital myasthenic syndrome, shown by mutations in *SETX*, *SIGMAR1* and *SLC5A7* (Chen *et al.*, 2004; Munch *et al.*, 2004; Al-Saif *et al.*, 2011; Salter *et al.*, 2018). Similarly, overlap with CNS diseases was shown for *AARS* mutations, which are also known to cause early-onset epileptic encephalopathy (Simons *et al.*, 2015).

SPTAN1 is a gene initially associated with a spectrum of epilepsy phenotypes (Syrbe *et al.*, 2017). Currently, 36 individuals with 24 different dominant *SPTAN1* variants have been reported, of which 11 are missense variants, 10 are in-frame deletions/duplications, two are truncating mutation and one is a splice variant (Syrbe *et al.*, 2017; Gartner *et al.*, 2018). More recently, mutations in *SPTAN1* have been described in patients with complex neurodevelopmental phenotypes (Gartner *et al.*, 2018). Furthermore, microdeletions encompassing one or more genes including *SPTAN1* and *STXBP1*, another causal epilepsy gene, have been reported to be responsible for complex phenotypes with combinations of early-onset primary dystonia, epilepsy, and intellectual disability (Stamberger *et al.*, 2016; Syrbe *et al.*, 2017).

Here, we describe three families with dominantly inherited HMN carrying different heterozygous *SPTAN1* nonsense variants identified by NGS. These families show great variability in clinical severity and these mutations are incompletely penetrant in at least two individuals. Because of the nature of the mutations and the loss of protein expression in mutation carriers, we suspect a mechanism of haploinsufficiency of αII-spectrin could be causative for the HMN phenotype.

Materials and methods

Genetic studies

DNA and lymphoblast extraction was performed on peripheral blood samples obtained from patients and family members after informed consent. All experiments described were approved by the ethical committee of the University of Antwerp. DNA for next generation sequencing was enriched for target regions using the Nextera Rapid Capture Expanded Exome kit (62 Mb) with the prepared library sequenced on an Illumina HiSeq 2500. Data annotation and variant filtering were performed using the Clinical Sequence Analyzer and Miner (Wuxi NextCODE). Either whole-genome (Families A and C) or whole-exome (Family B) sequencing was performed on Individuals A:I:1, A:II:2, A:III:1, B:II:2, B:III:2, B:IV:1, C:III:2 and C:III:3 (Fig. 1A–C).

Variants in known genes for inherited peripheral neuropathy, ALS, myopathy, ataxia and hereditary spastic paraplegia were investigated first. Non-synonymous, in-frame deletions/insertions and predicted loss-of-function variants with a population frequency of $<0.5\%$ and CADD >20 were withheld for follow-up by dideoxy sequence analysis (Rentzsch *et al.*, 2019). As no segregating variants in known genes were present, the same filtering was used on all protein-coding genes. Upon identification of the *SPTAN1* variants, co-segregation with the phenotype within each family was confirmed using dideoxy sequence analysis. Primer sequences are available upon request.

We performed subsequent targeted panel sequencing of *SPTAN1* on an additional 95 HMN patients, which revealed no additional causal variants in *SPTAN1*, indicating that *SPTAN1* loss-of-function mutations are rare.

Genome-wide significance testing

We calculated the significance of finding three inherited loss-of-function mutations in our HMN NGS cohort consisting of 73 families, by using a python-based version of SORVA software (Rao and Nelson, 2018).

Heterozygous loss-of-function variants in *SPTAN1* in the general population with a minor-allele frequency <0.05 as queried by SORVA results in a frequency of 0.0. Further calculations were not possible using this frequency. Therefore, we used a frequency of 3.13×10^{-4} as determined by all predicted loss-of-function mutations present in gnomAD, including variants with loss-of-function flags (Lek *et al.*, 2016).

Subsequently, we subdivided our cohort into groups with different coefficients of relationships: 1 for index pairs, 0.5 for index/parent pairs and 0.25 for sibling pairs and tri-

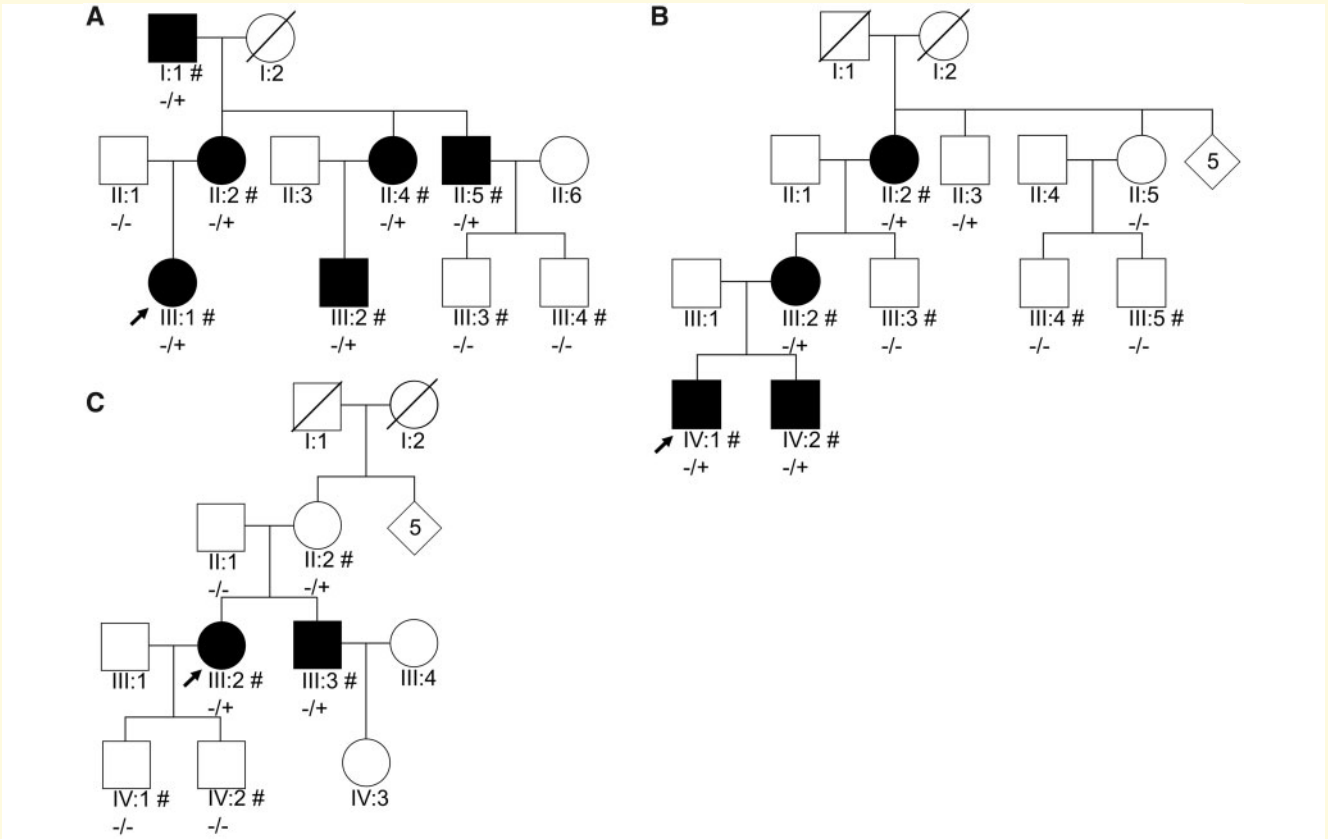

Figure 1 Pedigrees of families with *SPTAN1* mutations. (**A**–**C**) Pedigrees of Families A–C with their respective mutation segregation of variants (NM_003127: c.415C > T), (NM_003127: c.4615C > T) and (NM_003127: c.6385C > T) showing affected (black), and unaffected (white) individuals. Those clinically and genetically investigated are indicated by a hash symbol and a mutation result, carrier (+/–) and non-carrier (–/–), respectively.

generational families. The calculated *P*-value was adjusted by Bonferroni correction and multiplied by the number of genes sequenced, which for NGS is 24 000.

Preparation of patient lymphoblasts

Patient lymphoblast cell lines were cultured in RPMI 1640 medium with 10% foetal bovine serum (FBS), 1% L-glutamine, 1% penicillin/streptomycin and 1% sodium pyruvate and maintained at 37°C with 6% CO_2. To assess nonsense-mediated decay (NMD) parallel split cells from the same patient were exposed to cycloheximide (100 ng/µl in dimethyl sulphoxide (DMSO)] or DMSO incubated for 4 h at 37°C. Another, parallel split of cells was kept untreated. Cycloheximide experiments were performed three consecutive times.

Dideoxy sequencing for assessment of nonsense-mediated decay of mutated allele

Primers for cDNA amplification of the three mutations were designed, sequences are available upon request. Messenger RNA extraction from lymphoblast cell pellets treated with cycloheximide, DMSO or non-treated was performed by RNeasy® mini kit (Qiagen). Subsequently, DNase treatment (Ambion) and cDNA synthesis was performed by SuperScript™ III (Thermo Fisher Scientific) according to manufacturer's protocol. PCR amplification of cDNA was performed using Titanium® Taq DNA polymerase (Takarabio) according to manufacturer's protocol.

Western blotting

For western blot, untreated lymphoblast cell pellets were treated with RIPA lysate buffer, containing protease and phosphatase inhibitors. Protein concentration was measured by BCA assay kit (Invitrogen) according to the manufacturer's protocol. Ten micrograms per sample were loaded onto a NuPAGE® 4–12% gradient Bis-Tris SDS-PAGE gel (Thermo Fisher Scientific), SeeBlue® Plus2 prestained ladder (Thermo Fisher Scientific) was used as a size reference. Wet transfer was performed onto nitrocellulose blotting paper. Subsequent blocking was performed using 5% skimmed milk powder in phosphate-buffered saline with Tween (PBST). A primary mouse anti-SPTAN1 antibody (1:1000) was used (Abcam ab11755). A rabbit-anti-mouse IgG2b HRP-conjugated secondary antibody was used. Stripping and reprobing for GAPDH (Genetex GTX100118 1:10 000) was performed to

assess equal loading across all samples. For each blot a new lysate was used.

Quantification using ImageJ over six different western blots, was performed measuring the band density. All quantifications were performed on 16-bit images with signals in the linear range and did not contain saturated bands. SPTAN1 expression was normalized by GAPDH expression per sample per blot. GAPDH-normalized SPTAN1 expression levels are plotted per individual.

Triton™ X-100 solubility assay

Primary lymphoblasts of three affected (Individuals A:III:1, B:IV:I, C:III:2) and three control (Individuals A:III3, B:III:3, C:IV:1) individuals were cultured as described previously. Cells (10×10^6) were pelleted and lysed with the following lysis buffer [50 mM Tris-HCL (pH 7.5), 150 mM NaCl, 5 mM EDTA and 1% Triton™ X-100 (v/v) with protease inhibitors (Life Technologies)] on ice for 20 min. Subsequent centrifugation at 14 000 rpm for 10 min at 4°C resulted in a soluble and insoluble fraction. The insoluble fraction was resuspended and sonicated with 10×1-s bursts at 50% amplitude and 0.6 pulse rate. Twenty micrograms of protein were loaded NuPAGE® 4–12% gradient Bis-Tris SDS-PAGE gel (Thermo Fisher Scientific), SeeBlue® Plus2 prestained ladder (Thermo Fisher Scientific) was used as a size reference. Western blotting proceeded as described previously. α-Tubulin (ab7291 1:5000) staining was performed as a loading control.

Preparation of patient fibroblasts

Fibroblasts were obtained from skin biopsies from the probands of Families A–C (Individuals A:III:1, B:IV:1 and C:III:2). For all fibroblast experiments an unrelated control fibroblast cell line was used. Fibroblast cultures were maintained in Dulbecco's modified Eagle medium high glucose (Thermofisher) with 10% FBS, 1% penicillin/streptomycin and 1% L-Glutamine and kept at 37°C and 5% CO_2.

Immunocytochemistry

Fibroblasts were seeded onto a Sensoplate™ 96-well plate with lid (Greiner) at 5×10^3 cells per well. Cells were incubated over night at 37°C and 5% CO_2. Cells were then fixed in 4% paraformaldehyde and blocked at room temperature with normal goat serum (1:500) in PBT (sterile PBS with 0.5% v/v Triton™ X-100 and 0.5% w/v BSA). Overnight incubation at 4°C with a primary mouse anti-SPTAN1 (1:200) (ab11755) and room temperature incubation with a goat-anti-mouse 488 Alexa Fluor® secondary antibody were performed. Subsequently, F-actin staining was performed with Alexa Fluor® 594-conjugated phalloidin (1.5 units/ml, 30 min, Life Technologies) and Hoechst 33342 nuclear staining was applied (1 µg/ml, 20 min Life Technologies). Image stacks (1024×1024 pixels; pixel size 130 nm × 130 nm) comprising the entire cell depth were taken with a Zeiss LSM700 confocal microscope using a 40×/1.30 Plan Neofluar® objective. Possible cross-talk of the fluorescence channels was excluded by using frame-by-frame scanning. Maximum intensity projections and image crops were made with ImageJ2 (Rueden *et al.*, 2017).

Data availability

The raw NGS data supporting the findings in patients cannot be made publicly available for confidentiality reasons. All other data generated or analysed during this study are included herein and in the Supplementary material.

Results

Genetic findings

We performed whole-exome or whole-genome sequencing in a cohort of 73 families with HMN. Initial analysis of variants in genes with known associations with neuropathy or related neuromuscular disorders identified no segregating variants in NGS performed on three individuals in Family A (Individuals A:I:1; A:II:2 and A:III:1), three affected individuals in Family B (Individuals B:II:2, B:III:2 and B:IV:1) and two affected siblings in Family C (Individuals C:III:1 and C:III:2). Subsequent analysis of all segregating variants in protein coding genes yielded nonsense mutations in *SPTAN1* in all three families: Family A (NM_003127: c.415C>T p.R139*), Family B (NM_003127: c.4615C>T p.Q1539*) and Family C (NM_003127: c.6385C>T p.Q2149*). Based on prediction scores, the absence of the variant in population databases gnomAD and ExAC, the predicted high intolerance for loss-of-function mutation, and the segregation of the variant within the NGS data, these *SPTAN1* variants are the most likely cause for the HMN phenotype in these families (Supplementary Table 2) (Lek *et al.*, 2016).

Subsequently, all variants were confirmed by dideoxy sequence analysis and found to co-segregate within each family consistent with autosomal dominant transmission (Fig. 1A–C). Identification of three loss-of-function variants in our HMN cohort consisting of 73 families reaches genome-wide significance as calculated using SORVA ($P = 6.2 \times 10^{-5}$) (Rao and Nelson, 2018).

Clinical findings

The patients carrying heterozygous *SPTAN1* nonsense mutations presented here, show lower limb weakness as result of a length-dependent motor neuropathy. In general, the phenotype is a juvenile onset slowly progressive axonal motor neuropathy (Table 1). However, the clinical phenotype is highly variable both inter- and intrafamilially, mainly in terms of severity (Table 1). As such, there are two possibly asymptomatic carriers, Individuals B:II:3 and C:II:2. Individual B:II:3 was clinically examined, but showed no indications for an axonal motor neuropathy phenotype, no EMG or nerve conduction studies (NCS) were performed. Individual C:II:2 was not clinically evaluated, based on hearsay she does not suffer from a motor neuropathy. It could be that Individual C:II:2 is mosaic for the mutation and does not carry the mutation in the tissues

Table 1 Overview of clinical findings

	Family A						Family B				Family C	
	A:I:1	A:II:2	A:II:3	A:II:4	A:III:1	A:III:2	B:II:2	B:III:2	B:IV:1	B:IV:2	C:III:2	C:III:3
Mutation	NM_003127: c.415C>T p.R139*						NM_003127: c.4615C>T p.Q1539*				NM_003127: c.6385C>T p.Q2149*	
Age at onset	<20 y	30 y	~30 y	<20 y	6 y	~12 y	Unknown	Childhood	3 y	3 y	9 y	12 y
Initial symptoms	Gait instability steppage gait	Easily sprained ankles	Gait instability	Slight weakness of right leg	Gait instability, easily sprained ankles	Drop toes	Unknown	Clumsiness	Steppage gait, lower limb weakness	Difficulty to walk on heels	Walking difficulties	Walking difficulties
Progression	Slow progression	No progression	No progression	No progression	Slow progression	No progression	No progression	No progression	Slow progression	Slow progression	Slow progression	Slow progression
Initial diagnosis at referral	Distal axonal neuropathy	Distal axonal neuropathy	-	-	Distal axonal neuropathy	-	Distal SMA	Distal SMA	Distal SMA	Distal SMA	Distal motor neuropathy	Distal motor neuropathy
Age at last examination	85 y	58 y	53 y	46 y	29 y	26 y	71 y	43 y	19 y	11 y	59 y	52 y
Sensory involvement	-	-	Slight reduction in vibration sense	-	Slight reduction in vibration sense	Slight reduction in vibration sense	-	-	-	-	Mild touch hypo-aesthesia	-
Gait	Wheelchair bound	Easily sprained ankles	Gait instability	Slight weakness of right leg	Drop toes, frequent falls	Drop toes	No heel walking	No heel walking	Steppage gait, no heel walking	Steppage gait, no heel walking	Steppage gait	Steppage gait
UL atrophy	-	-	-	-	-	-	-	-	-	-	Mild	Mild
UL weakness	-	-	-	-	-	-	-	-	-	-	Mild	Mild
UL reflexes	Reduced	Normal	Normal	Normal	Normal	Normal	Normal	Normal	Normal	Normal	Reduced	Reduced
LL atrophy	Distal leg and foot intrinsics	-	-	-	Distal leg and foot intrinsics	-	Calf atrophy	Calf atrophy	Moderate distal	-	Moderate distal	Severe distal
LL weakness	4/5 distal	4/5 toe extensors	4/5 toe extensors	2–4/5 in toe extensors	0–2/5 toe extensors	2–4/5 toe extensors	Mild distal (4/5)	Mild distal (4/5)	Mild distal (4/5)	1–2/5 toe extensor, PL 3/5 TA 2/5	4/5 toe extensor and distal leg	4/5 toe extensor and distal leg
LL reflexes	Absent	Reduced	Reduced	Reduced	Normal	Normal	Normal	Normal	Reduced	Reduced	Absent	Absent
Foot deformity	-	Hammer toes	Hammer toes, hallux valgus	-	-	Hammer toes, hallux valgus	Flat feet and claw toes	Flat feet	-	Hallux valgus	Pes cavus, hammer toes	Pes cavus, hammer toes
Additional clinical features	Requires orthopaedic insoles	Requires orthopaedic insoles	-	-	Restless legs	-	-	Requires orthopaedic insoles	Short Achilles tendon	Requires orthopaedic insoles	Short Achilles tendon	-
NCS/EMG	N/P	Mild motor axonal neuropathy	Mild motor axonal neuropathy	N/P	Motor axonal neuropathy	Motor axonal neuropathy	Motor axonal neuropathy	Motor axonal neuropathy	Motor predominant axonal neuropathy	Motor predominant axonal neuropathy	Motor predominant axonal neuropathy	Motor axonal neuropathy

(–) = negative/absent; (+) = positive; EMG = electromyography; LL = lower limb(s); N/P = not performed, weakness reported in MRC scale; PL = M. peroneus longus; SMA = spinal muscular atrophy; TA = M. tibialis anterior; UL = upper limb(s).

affected in a neuropathy phenotype. DNA was extracted from hair and buccal swap from Individual C:II:2. Dideoxy sequencing showed the presence of the mutation in both hair, blood and buccal sample, thus we could not confirm Individual C:II:2 as a mosaic carrier.

As there was an existing association between *SPTAN1* mutations and epilepsy, we considered the possibility of our patients showing a similar phenotype in addition to the HMN phenotype. However, unlike patients previously described with heterozygous *SPTAN1* mutations, none of the individuals in this study showed symptoms or signs of epilepsy, intellectual disability and hearing or visual loss, as such no formal investigations were performed. All individuals examined had normal school and professional careers and were capable to start families, none of the patients were care-dependent or living in residential facilities. Since no brain MRIs were performed, structural (asymptomatic) brain abnormalities cannot be excluded. With exception of Individual B:III:2, who takes levothyroxine to treat a postpartum subclinical hypothyroidism, there were no indications for a thyroid abnormality as previously identified in two patients (Table 1) (Gartner *et al.*, 2018).

Family A

The first family's proband (Individual A:III:1; Fig. 1A) presented with early-onset gait difficulties from the age of 6 years, resulting in easily sprained ankles and frequent falls. She has a bilateral toe drop and is unable to walk on the heels. The overall progression is slow as the patient is able to walk unaided at the age of 30 years. She has atrophy of the intrinsic foot muscles and slight atrophy of the lower legs. Reflexes in both lower and upper limbs are normal. NCS showed normal motor and sensory conduction velocities and slightly decreased compound muscle action potentials, fitting with a distal length-dependent axonal neuropathy (Supplementary Table 1).

The mother of the proband (Individual A:II:2) is less affected, although she mentions similarly frequent sprained ankles and frequent falls. She has a limited ability to walk on the heels and a slight bilateral toe drop but remains ambulatory at age 59 years. The grandfather of the proband (Individual A:I:1) was previously diagnosed with axonal neuropathy. While the grandfather is now wheelchair-bound due to a hip fracture after a fall, he previously struggled with gait difficulties but had been ambulatory until age 62. The proband's aunt (Individual A:II:4), uncle (Individual A:II:5) and cousin (Individual A:III:2) all reported no symptoms before clinical investigation, but upon inspection show slightly decreased strength of the foot dorsiflexors and a toe drop.

Family B

The second family's proband (Individual B:IV:1; Fig. 1B) presented with early-onset gait difficulties from the age of 3 years, with weakness in the lower limbs, and a mildly shortened Achilles tendons. He reported no sensory involvement. The deep tendon reflexes were reduced in the lower limbs and normal in the upper limbs. The NCS indicated a neurogenic rather than myogenic disorder and showed findings fitting with an axonal motor predominant neuropathy. The proband was initially diagnosed as a patient with distal SMA. Both the proband's mother (Individual B:III:2) and grandmother (Individual B:II:2) were mildly affected and showed weakness of dorsal extension with preserved reflexes, pes planus and calf hypotrophy. Both underwent NCS, which showed results compatible with neuronal degradation indicative of pure motor axonal neuropathy mainly affecting the lower limbs (Supplementary Table 1). Most recently, Individual B:IV:2, the younger brother of the proband (Individual B:IV:1) showed weakness in the lower limbs, presenting as an inability to walk on heels starting at the age of 3 years. He shows no weakness in the upper limbs. An NCS performed at age 5, showed findings compatible with a motor predominant axonal neuropathy. None of the members of the family showed pyramidal symptoms (Supplementary Table 1).

Family C

The third proband (Individual C:III:2; Fig. 1C) presented with walking difficulties from the age of 9 years, with inability to run and frequent falls. Shortly after, she underwent orthopaedic surgery to correct a bilateral Achilles tendon shortening. The motor difficulties progressed very slowly and the patient is able to walk at age 59 with a cane, but with a marked steppage gait. Deep tendon reflexes are absent in the lower limbs and reduced in the upper limbs. Distal leg hypotrophy is evident. In the past 2 years, mild weakness and atrophy of the hands and distal arm muscles was observed. She reports mild touch hypoesthesia and reduced dexterity. NCS in this patient support a distal axonal motor predominant neuropathy (Supplementary Table 1).

The proband's younger brother (Individual C:III:3) showed similar walking difficulties from the age of 12 years, but is able to walk unaided at the age of 52. The non-consanguineous parents reported no motor disabilities at age 93 and 87 years old. The proband has two children (Individuals C:IV:1 and C:IV:2) of 38 and 34 years, respectively, who both have a normal phenotype.

SPTAN1 nonsense mutations cause loss-of-expression

SPTAN1 (NM_003127) comprises 56 exons encoding the 2472 amino acid long wild-type αII-spectrin protein. The αII-spectrin protein (SPTAN1) is a major component of the spectrin skeleton where it forms antiparallel tetramers made of heterodimers of two αII and two β-spectrin units. A single αII-spectrin protein consists of 20 spectrin repeats, a SH3 domain and two EF hand domains. The C-terminal spectrin repeats are coiled coils involved in dimerization with β-spectrin, whereas the two EF-hand domains are thought to be able to interact and modulate the actin-

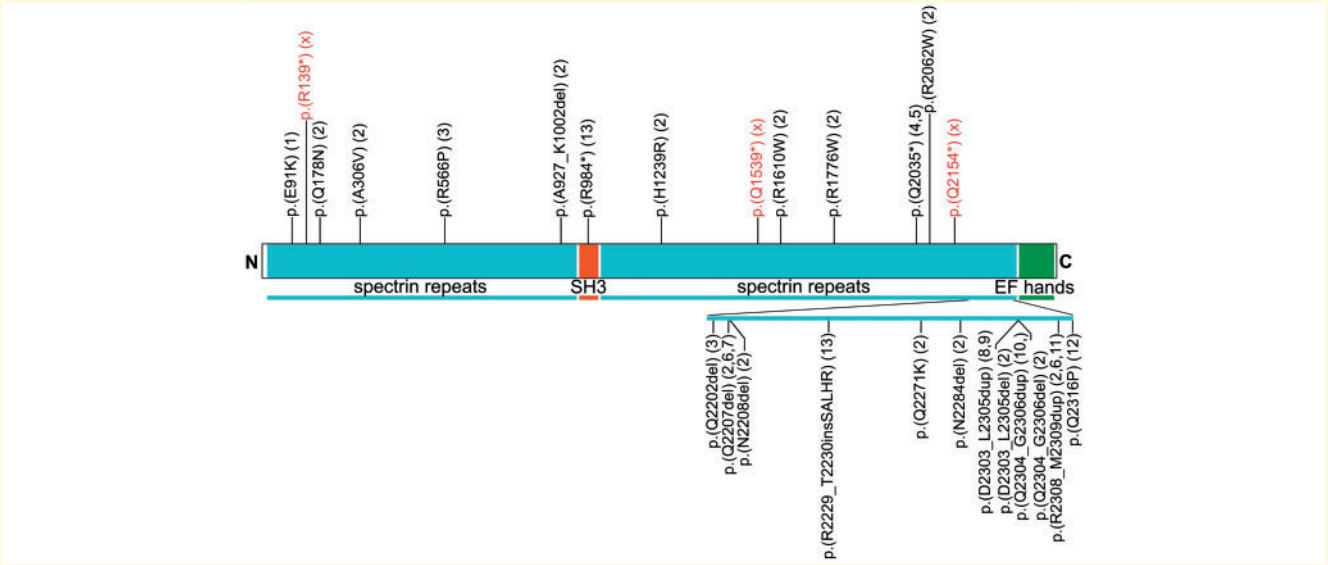

Figure 2 Graphical representation of *SPTAN1* with mutations identified in epilepsy and HMN patients. Graphical representation of SPTAN1 protein wherein all previously reported *SPTAN1* mutations have been indicated with their reference between brackets as well as the hereditary motor neuropathy-associated mutations discussed in this study indicated in red and by (x). Previously reported mutation as identified by: 1, Gilissen *et al.* (2014); 2, Syrbe *et al.* (2017); 3, Hamdan *et al.* (2012); 4, Yavarna *et al.* (2015); 5, Retterer *et al.* (2016); 6, Saitsu *et al.* (2010); 7, Writzl *et al.* (2012); 8, Nonoda *et al.* (2013); 9, Tohyama *et al.* (2015); 10, Ream and Mikati (2014); 11, Rapaccini *et al.* (2018); 12, Stavropoulos *et al.* (2016); and 13, Gartner *et al.* (2018).

binding domains of the β-spectrin (Broderick and Winder, 2005; Machnicka *et al.*, 2014). Mutations causing epilepsy and HMN do not seem to be linked to specific regions or domains of the protein, although the C-terminus seems enriched for in-frame deletions and insertions (Fig. 2). A recent study by Gartner *et al.* (2018) identified a nonsense mutation in a patient without epilepsy and hypothesized a haploinsufficiency mechanism. To investigate whether the nature of these nonsense mutations indeed results in a haploinsufficiency of αII-spectrin, we performed expression studies on mRNA and protein level by PCR and Sanger sequencing and western blot respectively.

We assessed whether the mutant mRNA is broken down by the NMD pathway by exposing patient lymphoblast to cycloheximide inhibiting the NMD pathway (Durand *et al.*, 2007). DMSO was used as a vehicle control. In the non-treated samples, the mutant allele is only slightly present, indicating an almost complete breakdown of the allele (Fig. 3). Inhibition of the NMD pathway by cycloheximide shows an increased presence of the mutant allele, confirming that the breakdown of the mutant allele under basal conditions is due to the NMD pathway activity (Fig. 3). These results are similar for all three mutations, confirming a similar mechanism despite different mutational locations.

In addition, we assessed expression on protein level by means of western blot of patient and control lymphoblast whole-cell lysates. Comparing protein expression between patient and controls of the same family we observed a clear decrease of wild-type αII-spectrin expression in patients lymphoblasts, but again not in their unaffected family members (Fig. 4A and B). No additional bands of other sizes, besides the expected αII-spectrin cleavage product at 150 kDa were observed.

αII-Spectrin nonsense mutations do not impact protein solubility or localization

To assess the differences between the previously reported mutations and our nonsense mutations, we investigated the soluble and insoluble fractions αII-spectrin by western blot as well as the presence and localization of aggregate formation of αII-spectrin in patients carrying *SPTAN1* nonsense mutations.

Both for the patient (Individuals A:III:1, B:IV:1, C:III:2) and control (Individuals A:III:3, B:III:3, C:IV:1) lymphoblast cell lines αII-spectrin was mainly present in the soluble fractions, although there was a clear insoluble αII-spectrin fraction present in all cell lines. We observed no enrichment of αII-spectrin in the insoluble fraction for any of the cell lines (Fig. 4C).

Next, we assessed the localization of αII-spectrin in patient (Individuals A:III:1, B:IV:1 and C:III:2) and unrelated control fibroblasts by immunocytochemistry. No differences were detected between patients and the control cells (Fig. 4D). Most αII-spectrin was present in small puncta spread over the cytoplasm. In addition, plasma membrane zones with increased αII-spectrin intensity could be observed in all samples. No αII-spectrin aggregates could be detected.

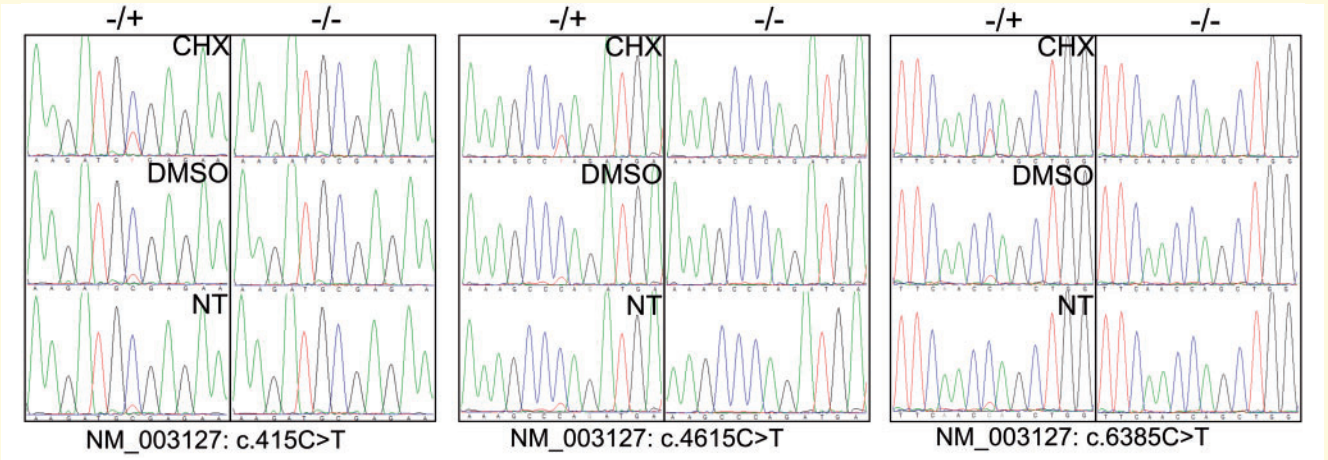

Figure 3 *SPTAN1* assessment of nonsense-mediated decay and mRNA. Mutation carrier (+/−) and non-carrier (−/−) sanger sequencing traces per mutation (NM_003127: c.415C>T), (NM_003127: c.4615C>T) and (NM_003127: c.6385C>T) showing effect of cycloheximide (CHX) and DMSO (vehicle control) treatment on mRNA breakdown of mutant allele in comparison to basal conditions depicted by the non-treated (NT) samples. Representative images of three independent experiments are shown.

Discussion

In this study we identified three nonsense mutation in *SPTAN1* by means of NGS in three unrelated families with an inherited peripheral motor neuropathy phenotype. The first family (Family A) consists of a proband, her affected mother, grandfather, aunt, uncle and cousin all carrying the p.(R139*) mutation. In this family, all affected individuals share symptoms of frequent falls and sprained ankles, as well as bilateral toe-drop and atrophy of intrinsic foot muscles to varying degrees. These symptoms and the NCS in the proband and cousin, support a mild length-dependent axonal motor neuropathy or HMN.

The second family (Family B) consists of a proband, and his affected bother, mother and grandmother with an HMN phenotype, who carry a p.(Q1539*) mutation. In this family the phenotype consists of lower limb weakness, in some individuals combined with reduced reflexes, and electrophysiological findings supporting a length-dependent axonal motor predominant neuropathy in different degrees of severity.

The third family (Family C) consists of a proband and her affected brother. They both carry the p.(Q2129*) mutation. For this family the phenotype is characterized by (early) childhood onset gait difficulties with inability to walk on the heels. Mild distal weakness of the upper limbs was noted in the eldest patient. Clinical findings in this family are consistent with a length-dependent axonal motor neuropathy. Interestingly, none of the described patients show any clinical signs of epilepsy, intellectual disability or ataxia, symptoms previously associated with other heterozygous *SPTAN1* mutations (Syrbe *et al.*, 2017; Gartner *et al.*, 2018).

Although the mutations segregate appropriately for an autosomal dominant disorder within each family, there are several individuals with mild phenotypes and possibly two asymptomatic carriers, which suggests variable penetrance of these mutations. In similar fashion, the gnomAD database contains a number of predicted loss-of-function variants, but still predicts very high loss-of-function intolerance for *SPTAN1* indicated by a pLi score of 1.0 and an *oe*-score of 0.06 (observed versus expected variants ratio) (Lek *et al.*, 2016). It is conceivable that the individuals in gnomAD are only mildly affected or asymptomatic as reduced penetrance is not novel in patients with heterozygous loss-of-function mutations (Cooper *et al.*, 2013). This also applies to *SPAST*, in which loss-of-function mutations are known to cause familial spastic paraplegia, with prominent variation in severity as well as reduced penetrance (Shoukier *et al.*, 2009). Even for *SCN1A* in which loss-of-function mutation are a well-known cause linked to the severe early-onset phenotype Dravet syndrome, several predicted loss-of-function mutations are present in gnomAD (Claes *et al.*, 2001). Therefore, some degree of caution is warranted when querying such databases.

Previously, *SPTAN1* mutations have been associated with a spectrum of epilepsy phenotypes (Syrbe *et al.*, 2017). Several *SPTAN1* missense and in-frame deletions/insertions are disease causing in a putative dominant-negative fashion indicated by SPTAN1 aggregates (Syrbe *et al.*, 2017). The presence of aggregates in some epilepsy patients with in-frame deletion or insertions seems to be an effect limited to specific mutations in the C-terminal region and not a universal characteristic for all *SPTAN1* mutations as indicated by our results and a recent report (Syrbe *et al.*, 2017; Gartner *et al.*, 2018). This would fit with the current understanding that especially C-terminal spectrin repeats are important for β-spectrin heterodimerization (Broderick and Winder, 2005). However, as these aggregates are only prominent in C-terminal mutations (and absent in one

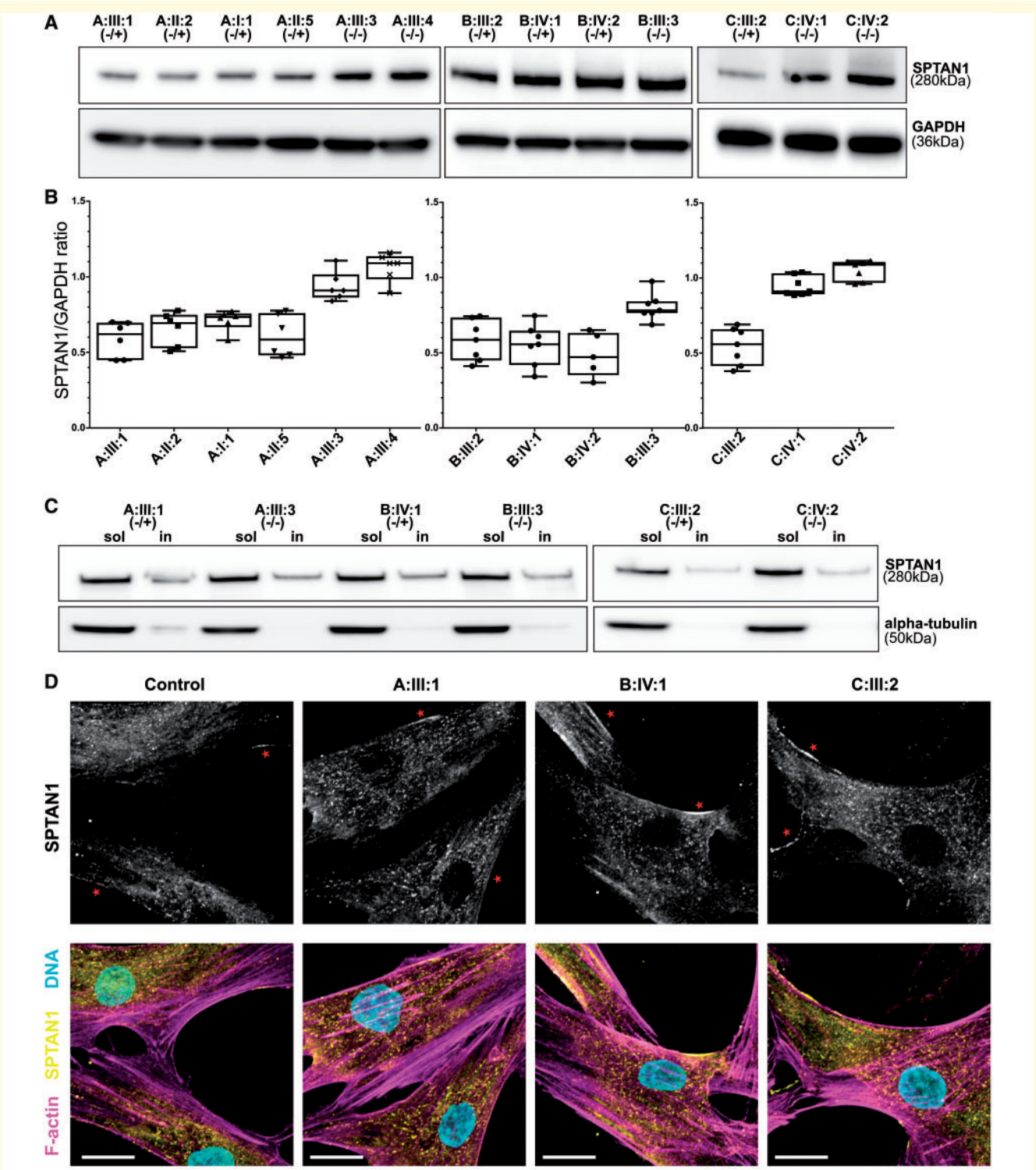

Figure 4 Comparison of SPTAN1 protein expression, solubility and staining pattern in patients versus controls. (**A**) Protein expression on western blot probing for SPTAN1 and GAPDH (loading control) (cropped images) of mutation carriers (+/–) and non-carriers (–/–), respectively. (**B**) Box-and-whisker plot representation of GAPDH normalized SPTAN1 expression levels per individual. *x*-axis represents SPTAN1 expression values normalized for GAPDH per individual. Error bars represent the minimal and maximal observed values and median and lower and upper quartile shown. (**C**) Soluble (sol) and insoluble (in) protein fractions per individual with western blot probing for SPTAN1 and actin (loading control) (cropped images), for mutation carriers (+/–) and non-carriers (–/–), respectively (**D**) Immunocytochemical staining of αII-spectrin in cultured skin fibroblasts of a healthy non-related control and of three patients, each carrying a different HMN causing mutation (Individuals A:III:1, B:IV:1 and C:III:2). Hoechst 33342 staining for the nucleus (cyan) and fluorophore-conjugated phalloidin staining for F-actin (magenta) was performed to counterstain αII-spectrin (yellow). Stars indicate clear stretches of αII-spectrin accumulations at the plasma membrane. Scale bar = 20 μm.

tested missense variant and nonsense variants), further investigation is needed to know if these aggregates are associated with all types of mutations in the C-terminal region and whether this correlates with the phenotypes identified in patients. It would be of special interest to see if β-spectrin function would be impaired due to the formation of these aggregates and the putative loss of stability (Saitsu *et al.*, 2010), as β-spectrin loss in *Drosophila melanogaster* results in a more severe phenotype than loss of α-spectrin. This may in turn translate to the more severe developmental phenotype observed in patients with C-terminal mutations in *SPTAN1* (Pielage *et al.*, 2005).

Recently, mutations in *SPTAN1* have been associated with a complex phenotype including intellectual disability, hypoplastic brain structures and fine and gross motor impairments without epilepsy (Gartner *et al.*, 2018). Gartner *et al.* suggest a loss of wild-type mRNA and haploinsufficiency mechanism for their nonsense mutant and demonstrate that fibroblasts in this patient have reduced wild-type levels of SPTAN1 protein. In our three families, we were able to show that these nonsense variants result in a mutant allele with premature stop codon, which is mostly degraded on mRNA level by means of NMD. In addition, we observe 60–80% αII-spectrin protein expression in patients when compared with controls, higher than the expected 50%, possibly indicating some degree of expression compensation by increased wild-type translation. Interestingly, expression levels of SPTAN1 protein do not seem to correlate with the intrafamilial or interfamilial differences in disease severity in the limited number of families investigated in this study.

In the past, multiple neurodevelopmental patients with microdeletions in the 9q34.11 region have been reported and these deletions often span multiple dosage-sensitive genes resulting in a contiguous gene deletion syndrome (Saitsu *et al.*, 2010; Campbell *et al.*, 2012). However, microdeletions encompassing the region with *SPTAN1*, do not necessarily give rise to an epilepsy phenotype, as indicated by several patients with a deletion that does not include *STXBP1*, and who do not have an epilepsy phenotype (Campbell *et al.*, 2012). This supports the belief that specific loss of *SPTAN1*, as seen in these HMN patients and the patients described by Gartner *et al.*, can be causal for a phenotype without epilepsy (Gartner *et al.*, 2018). Currently, no whole gene deletions of *SPTAN1* only have been described.

SPTAN1 plays an important role in stabilizing the spectrin-dependent cytoskeleton and the definition of nodal, paranodal and juxtaparanodal membrane domains in neurons (Pielage *et al.*, 2005; Huang *et al.*, 2017*a*). While the spectrin skeleton is abundantly present in both the peripheral and central nervous system (Goodman *et al.*, 1995; Bennett and Baines, 2001), its role in the postembryonic nervous system is elusive. The role of the cytoskeleton in peripheral neuropathies is well known as mutations in multiple cytoskeletal associated proteins have been associated with inherited peripheral neuropathy, including DST (cytoskeleton linker protein), NEFL (intermediate filament for maintenance of cytoskeleton) and GAN (binds to microtubule-associated protein 1B) (Bomont *et al.*, 2000; Jordanova *et al.*, 2003; Edvardson *et al.*, 2012).

Deletion of orthologues to the αII-spectrin gene from *Drosophila*, *Caenorhabditis elegans* and *Mus musculus* lead to embryonic lethality, showing αII-spectrin is essential for cellular development and function (Lee *et al.*, 1993; Featherstone *et al.*, 2001; Norman and Moerman, 2002). Specific loss of presynaptic α-spectrin was shown to lead to increased synapse retractions in *Drosophila* neuromuscular junction including a larger number of boutons as well as disruption of retrograde transport (Pielage *et al.*, 2005). Both synapse retractions and disrupted retrograde transport have been reported for a number of genes causative for motor neuron disorders including; *DCNT1* and *SOD1* (ALS), and *DYNC1H1* (CMT) (Murakami *et al.*, 2001; Hafezparast *et al.*, 2003; Zhou *et al.*, 2016), supporting the conclusion that reduced αII-spectrin levels could be capable of inducing a degenerative synapse retraction, leading to the axonal degeneration causal in HMN (Massaro *et al.*, 2009).

Previously, specific loss of αII-spectrin in peripheral sensory neurons in mice was shown to have a length-dependent degenerative effect (Huang *et al.*, 2017*b*). The authors showed that the αII-spectrin-dependent cytoskeleton is dispensable for maintenance of small diameter axons but is essential for axon integrity in large diameter myelinated axons. Upon increased αII-spectrin levels, larger diameter axons could be protected from degeneration (Huang *et al.*, 2017*b*). Compared to the much shorter and thinner CNS axons, lower motor neurons might be more susceptible to damage, as the extraordinary length and larger diameter of their axons requires highly efficient processes of cellular signaling (Huang *et al.*, 2017*b*). It is therefore conceivable that large calibre lower motor neuron axons are sensitive to moderate reductions in overall αII-spectrin levels which could provide a potential explanation for the manifestation of an HMN phenotype upon nonsense mutations in *SPTAN1*. Also, the phenotype severity could be dependent upon the degree of reduction in protein expression levels. However, this requires further detailed investigation of more patients with various causal *SPTAN1* mutations, since it might be that they all have some degree of lower motor neuron degeneration. Especially in the severe syndromic phenotypes it might be that mild peripheral nervous system involvement is lost in the global severity of the clinical presentation.

A point of interest is that heterozygous *Spna2*/*SPTAN1* knockout mice do not seem to show a phenotype, therefore indicating that *SPTAN1* haploinsufficiency is tolerated in these animals (Stankewich *et al.*, 2011). While heterozygous (*Spna2*$^{+/-}$) mice were morphologically indistinguishable from wild-type animals, they also showed similar protein expression levels, which is unlike what we observe in heterozygous patients and this might influence the phenotypic outcome (Stankewich *et al.*, 2011; Gartner *et al.*, 2018). It is possible that there is a feedback loop

in mice, leading to increased Spna2 protein expression from the one wild-type allele. However, it is also known that not all genes that are intolerant to haploinsufficiency in humans prove to be so in mice, and finally the effect of the genetic background of the mice can also have a significant effect on the penetrance of many phenotypes. It is worth further investigating mice of different strains starting from the assumption that a pathological phenotype might only be present upon clear loss of Spna2 protein expression, since this would better model the situation in patients with *SPTAN1* nonsense mutations.

With the increased number of *SPTAN1* mutations identified and the ever-increasing phenotypic variability, it is clear that further systematic assessment of the mutational differences in αII-spectrin protein and mRNA levels as well as the possible underlying mechanisms (dominant-negative, gain-of-function and haploinsufficiency) is necessary. Such systematic studies should aim to look at the different mutations associated with the epilepsy spectrum, including the C-terminal in-frame deletions and insertions as well as missense mutations. Non-epilepsy mutations should include the milder HMN phenotype described here as well as the more complex developmental phenotype (Gartner *et al.*, 2018).

In conclusion, we present three families with dominantly inherited *SPTAN1* nonsense mutations and a hereditary motor neuropathy phenotype, expanding the *SPTAN1*-associated phenotype spectrum. This study corroborates nonsense mutations and partial loss of αII-spectrin as a mechanism causal for peripheral nervous system motor axon degeneration. In addition, we show that *SPTAN1* mutations do not always lead to phenotypes that include epilepsy and that disease severity can be highly variable. The exact pathomechanisms underlying the differences and similarities exhibited by *SPTAN1* mutations and phenotypes require further investigation.

Acknowledgements

We thank all the patients and family members for their participation in this study.

Funding

This work was supported by the Association Belge contre les Maladies Neuromusculaire (ABMM) - Aide à la Recherche ASBL (2017–2018/05) and the EU FP7/2007–2013 under grant agreement number 2012–305121 (NEUROMICS). J.B. is supported by a Senior Clinical Researcher mandate of the Research Fund - Flanders (FWO) under grant agreement number 1805016N.

Competing interests

The authors report no competing interests.

Supplementary material

Supplementary material is available at *Brain* online.

References

Al-Saif A, Al-Mohanna F, Bohlega S. A mutation in sigma-1 receptor causes juvenile amyotrophic lateral sclerosis. Ann Neurol 2011; 70: 913–9.

Bennett V, Baines AJ. Spectrin and ankyrin-based pathways: metazoan inventions for integrating cells into tissues. Physiol Rev 2001; 81: 1353–92.

Boerkoel CF, Takashima H, Garcia CA, Olney RK, Johnson J, Berry K, et al. Charcot-Marie-Tooth disease and related neuropathies: mutation distribution and genotype-phenotype correlation. Ann Neurol 2002; 51: 190–201.

Bomont P, Cavalier L, Blondeau F, Ben Hamida C, Belal S, Tazir M, et al. The gene encoding gigaxonin, a new member of the cytoskeletal BTB/Kelch repeat family, is mutated in giant axonal neuropathy. Nat Genet 2000; 26: 370–4.

Broderick MJ, Winder SJ. Spectrin, alpha-actinin, and dystrophin. Adv Protein Chem 2005; 70: 203–46.

Campbell IM, Yatsenko SA, Hixson P, Reimschisel T, Thomas M, Wilson W, et al. Novel 9q34.11 gene deletions encompassing combinations of four Mendelian disease genes: STXBP1, SPTAN1, ENG, and TOR1A. Genet Med 2012; 14: 868–76.

Chen YZ, Bennett CL, Huynh HM, Blair IP, Puls I, Irobi J, et al. DNA/RNA helicase gene mutations in a form of juvenile amyotrophic lateral sclerosis (ALS4). Am J Hum Genet 2004; 74: 1128–35.

Claes L, Del-Favero J, Ceulemans B, Lagae L, Van Broeckhoven C, De Jonghe P. De novo mutations in the sodium-channel gene SCN1A cause severe myoclonic epilepsy of infancy. Am J Hum Genet 2001; 68: 1327–32.

Cooper DN, Krawczak M, Polychronakos C, Tyler-Smith C, Kehrer-Sawatzki H. Where genotype is not predictive of phenotype: towards an understanding of the molecular basis of reduced penetrance in human inherited disease. Hum Genet 2013; 132: 1077–130.

Durand S, Cougot N, Mahuteau-Betzer F, Nguyen CH, Grierson DS, Bertrand E, et al. Inhibition of nonsense-mediated mRNA decay (NMD) by a new chemical molecule reveals the dynamic of NMD factors in P-bodies. J Cell Biol 2007; 178: 1145–60.

Edvardson S, Cinnamon Y, Jalas C, Shaag A, Maayan C, Axelrod FB, et al. Hereditary sensory autonomic neuropathy caused by a mutation in dystonin. Ann Neurol 2012; 71: 569–72.

Featherstone DE, Davis WS, Dubreuil RR, Broadie K. Drosophila alpha- and beta-spectrin mutations disrupt presynaptic neurotransmitter release. J Neurosci 2001; 21: 4215–24.

Gartner V, Markello TC, Macnamara E, De Biase A, Thurm A, Joseph L, et al. Novel variants in SPTAN1 without epilepsy: An expansion of the phenotype. Am J Med Genet A 2018; 176: 2768–76.

Gilissen C, Hehir-Kwa JY, Thung DT, van de Vorst M, van Bon BW, Willemsen MH, et al. Genome sequencing identifies major causes of severe intellectual disability. Nature 2014; 511: 344–7.

Goodman SR, Zimmer WE, Clark MB, Zagon IS, Barker JE, Bloom ML. Brain spectrin: of mice and men. Brain Res Bull 1995; 36: 593–606.

Hafezparast M, Klocke R, Ruhrberg C, Marquardt A, Ahmad-Annuar A, Bowen S, et al. Mutations in dynein link motor neuron degeneration to defects in retrograde transport. Science 2003; 300: 808–12.

Hamdan FF, Saitsu H, Nishiyama K, Gauthier J, Dobrzeniecka S, Spiegelman D, et al. Identification of a novel in-frame de novo mutation in SPTAN1 in intellectual disability and pontocerebellar atrophy. Eur J Hum Genet 2012; 20: 796–800.

Huang CY, Zhang C, Ho TS, Oses-Prieto J, Burlingame AL, Lalonde J, et al. AlphaII spectrin forms a periodic cytoskeleton at the axon initial segment and is required for nervous system function. J Neurosci 2017a; 37: 11311–22.

Huang CY, Zhang C, Zollinger DR, Leterrier C, Rasband MN. An alphaII Spectrin-based cytoskeleton protects large-diameter myelinated axons from degeneration. J Neurosci 2017b; 37: 11323–34.

Jordanova A, De Jonghe P, Boerkoel CF, Takashima H, De Vriendt E, Ceuterick C, et al. Mutations in the neurofilament light chain gene (NEFL) cause early onset severe Charcot-Marie-Tooth disease. Brain 2003; 126: 590–7.

Lee JK, Coyne RS, Dubreuil RR, Goldstein LS, Branton D. Cell shape and interaction defects in alpha-spectrin mutants of Drosophila melanogaster. J Cell Biol 1993; 123: 1797–809.

Lek M, Karczewski KJ, Minikel EV, Samocha KE, Banks E, Fennell T, et al. Analysis of protein-coding genetic variation in 60,706 humans. Nature 2016; 536: 285–91.

Machnicka B, Czogalla A, Hryniewicz-Jankowska A, Boguslawska DM, Grochowalska R, Heger E, et al. Spectrins: a structural platform for stabilization and activation of membrane channels, receptors and transporters. Biochim Biophys Acta 2014; 1838: 620–34.

Massaro CM, Pielage J, Davis GW. Molecular mechanisms that enhance synapse stability despite persistent disruption of the spectrin/ankyrin/microtubule cytoskeleton. J Cell Biol 2009; 187: 101–17.

Montenegro RM Jr, Costa-Riquetto AD, Fernandes VO, Montenegro A, de Santana LS, Jorge AAL, et al. Homozygous and heterozygous nuclear lamin A p.R582C mutation: different lipodystrophic phenotypes in the same kindred. Front Endocrinol (Lausanne) 2018; 9: 458.

Munch C, Sedlmeier R, Meyer T, Homberg V, Sperfeld AD, Kurt A, et al. Point mutations of the p150 subunit of dynactin (DCTN1) gene in ALS. Neurology 2004; 63: 724–6.

Murakami T, Nagano I, Hayashi T, Manabe Y, Shoji M, Setoguchi Y, et al. Impaired retrograde axonal transport of adenovirus-mediated E. coli LacZ gene in the mice carrying mutant SOD1 gene. Neurosci Lett 2001; 308: 149–52.

Nonoda Y, Saito Y, Nagai S, Sasaki M, Iwasaki T, Matsumoto N, et al. Progressive diffuse brain atrophy in West syndrome with marked hypomyelination due to SPTAN1 gene mutation. Brain Dev 2013; 35: 280–3.

Norman KR, Moerman DG. Alpha spectrin is essential for morphogenesis and body wall muscle formation in Caenorhabditis elegans. J Cell Biol 2002; 157: 665–77.

Pielage J, Fetter RD, Davis GW. Presynaptic spectrin is essential for synapse stabilization. Curr Biol 2005; 15: 918–28.

Rao AR, Nelson SF. Calculating the statistical significance of rare variants causal for Mendelian and complex disorders. BMC Med Genom 2018; 11: 53.

Rapaccini V, Esposito S, Strinati F, Allegretti M, Manfroi E, Miconi F, et al. A Child with a c.6923_6928dup (p.Arg2308_Met2309dup) SPTAN1 mutation associated with a severe early infantile epileptic encephalopathy. Int J Mol Sci 2018; 19: 1976.

Ream MA, Mikati MA. Clinical utility of genetic testing in pediatric drug-resistant epilepsy: a pilot study. Epilepsy Behav 2014; 37: 241–8.

Rentzsch P, Witten D, Cooper GM, Shendure J, Kircher M. CADD: predicting the deleteriousness of variants throughout the human genome. Nucleic Acids Res 2019; 47: D886–94.

Retterer K, Juusola J, Cho MT, Vitazka P, Millan F, Gibellini F, et al. Clinical application of whole-exome sequencing across clinical indications. Genet Med 2016; 18: 696–704.

Rossor AM, Kalmar B, Greensmith L, Reilly MM. The distal hereditary motor neuropathies. J Neurol Neurosurg Psychiatry 2012; 83: 6–14.

Rueden CT, Schindelin J, Hiner MC, DeZonia BE, Walter AE, Arena ET, et al. ImageJ2: ImageJ for the next generation of scientific image data. BMC Bioinform 2017; 18: 529.

Saitsu H, Tohyama J, Kumada T, Egawa K, Hamada K, Okada I, et al. Dominant-negative mutations in alpha-II spectrin cause West syndrome with severe cerebral hypomyelination, spastic quadriplegia, and developmental delay. Am J Hum Genet 2010; 86: 881–91.

Salter CG, Beijer D, Hardy H, Barwick KES, Bower M, Mademan I, et al. Truncating SLC5A7 mutations underlie a spectrum of dominant hereditary motor neuropathies. Neurol Genet 2018; 4: e222.

Shoukier M, Neesen J, Sauter SM, Argyriou L, Doerwald N, Pantakani DV, et al. Expansion of mutation spectrum, determination of mutation cluster regions and predictive structural classification of SPAST mutations in hereditary spastic paraplegia. Eur J Hum Genet 2009; 17: 187–94.

Simons C, Griffin LB, Helman G, Golas G, Pizzino A, Bloom M, et al. Loss-of-function alanyl-tRNA synthetase mutations cause an autosomal-recessive early-onset epileptic encephalopathy with persistent myelination defect. Am J Hum Genet 2015; 96: 675–81.

Stamberger H, Nikanorova M, Willemsen MH, Accorsi P, Angriman M, Baier H, et al. STXBP1 encephalopathy: A neurodevelopmental disorder including epilepsy. Neurology 2016; 86: 954–62.

Stankewich MC, Cianci CD, Stabach PR, Ji L, Nath A, Morrow JS. Cell organization, growth, and neural and cardiac development require alphaII-spectrin. J Cell Sci 2011; 124: 3956–66.

Stavropoulos DJ, Merico D, Jobling R, Bowdin S, Monfared N, Thiruvahindrapuram B, et al. Whole genome sequencing expands diagnostic utility and improves clinical management in pediatric medicine. NPJ Genom Med 2016; 1: 15012.

Syrbe S, Harms FL, Parrini E, Montomoli M, Mutze U, Helbig KL, et al. Delineating SPTAN1 associated phenotypes: from isolated epilepsy to encephalopathy with progressive brain atrophy. Brain 2017; 140: 2322–36.

Tazir M, Bellatache M, Nouioua S, Vallat JM. Autosomal recessive Charcot-Marie-Tooth disease: from genes to phenotypes. J Peripher Nerv Syst 2013; 18: 113–29.

Tohyama J, Nakashima M, Nabatame S, Gaik-Siew C, Miyata R, Rener-Primec Z, et al. SPTAN1 encephalopathy: distinct phenotypes and genotypes. J Hum Genet 2015; 60: 167–73.

Writzl K, Primec ZR, Strazisar BG, Osredkar D, Pecaric-Meglic N, Kranjc BS, et al. Early onset West syndrome with severe hypomyelination and coloboma-like optic discs in a girl with SPTAN1 mutation. Epilepsia 2012; 53: e106–10.

Yavarna T, Al-Dewik N, Al-Mureikhi M, Ali R, Al-Mesaifri F, Mahmoud L, et al. High diagnostic yield of clinical exome sequencing in Middle Eastern patients with Mendelian disorders. Hum Genet 2015; 134: 967–80.

Zhou B, Yu P, Lin MY, Sun T, Chen Y, Sheng ZH. Facilitation of axon regeneration by enhancing mitochondrial transport and rescuing energy deficits. J Cell Biol 2016; 214: 103–19.